

Feasibility of the Non-Window-Type 3D-Printed Porous Titanium Cage in Posterior Lumbar Interbody Fusion

A Randomized Controlled Multicenter Trial

Dae-Woong Ham, MD, Sang-Min Park, MD, Youngbae B. Kim, MD, Dong-Gune Chang, MD, Jae Jun Yang, MD, Byung-Taek Kwon, MD, and Kwang-Sup Song, MD

Background: Three-dimensionally printed titanium (3D-Ti) cages can be divided into 2 types: window-type cages, which have a void for bone graft, and non-window-type cages without a void. Few studies have investigated the necessity of a void for bone graft in fusion surgery. Therefore, the present study assessed the clinical and radiographic outcomes of window and non-window-type 3D-Ti cages in single-level posterior lumbar interbody fusion.

Methods: A total of 70 patients were randomly assigned to receive either a window or non-window cage; 61 patients (87%) completed final follow-up (32 from the window cage group, 29 from the non-window cage group). Radiographic outcomes, including fusion rates, subsidence, and intra-cage osseointegration patterns, were assessed. Intra-cage osseointegration was measured using the intra-cage bridging bone score for the window cage group and the surface osseointegration ratio score for the non-window cage group. Additionally, we looked for the presence of the trabecular bone remodeling (TBR) sign on computed tomography (CT) images.

Results: Of the 61 patients, 58 achieved interbody fusion, resulting in a 95.1% fusion rate. The fusion rate in the non-window cage group was comparable to, and not significantly different from, that in the window cage group (96.6% and 93.8%, $p > 0.99$). The subsidence rate showed no significant difference between the window and non-window cage groups (15.6% and 3.4%, respectively; $p = 0.262$). The intra-cage osseointegration scores showed a significant difference between the groups ($p = 0.007$), with the non-window cage group having a higher proportion of cases with a score of 4 compared with the window cage group. The TBR sign was observed in 87.9% of patients who achieved interbody fusion, with a higher rate in the non-window cage group across the entire cohort although the difference was not significant (89.7% versus 78.1%, $p = 0.385$).

Conclusions: Non-window-type 3D-Ti cages showed equivalent clinical outcomes compared with window-type cages and comparable interbody fusion rates. These results suggest that the potential advantages of 3D-Ti cages could be optimized in the absence of a void for bone graft by providing a larger contact surface for osseointegration.

Level of Evidence: Therapeutic Level II. See Instructions for Authors for a complete description of levels of evidence.

Posterior lumbar interbody fusion (PLIF) is a widely used surgical technique that has shown favorable outcomes in the treatment of various spinal disorders, including degenerative disc disease, spondylolisthesis, and spinal stenosis¹⁻³. The introduction of interbody cages has provided surgeons with a means to improve fusion rates and achieve desirable outcomes⁴⁻⁷.

The evolution of cage material began with solid titanium cages in the 1980s^{8,9}, offering high fusion rates but causing sub-

sidence due to their high elastic modulus^{10,11}. Polyetheretherketone (PEEK) cages were introduced to mitigate this issue because their elastic modulus is similar to that of cortical bone¹²⁻¹⁴. However, PEEK's biopassive nature hinders apatite formation, which is essential for osteoblastic differentiation^{15,16}. To address the issue of fibrous interface development at the vertebral end plate, which potentially causes implant micromotion¹⁷, a window-type cage with a void for bone graft was designed to enhance fusion rates^{12,18}.

Disclosure: No external funding was received for this study. The **Disclosure of Potential Conflicts of Interest** forms are provided with the online version of the article (<http://links.lww.com/JBJS/I182>).

A **data-sharing statement** is provided with the online version of the article (<http://links.lww.com/JBJS/I183>).

Subsequently, ceramic cages and titanium-coated PEEK cages were introduced to overcome issues with poor cage-bone osseointegration^{19,21}.

The recent advancement of 3D printing technology has facilitated the creation of 3D-printed porous titanium (3D-Ti) cages, improving their osteoinductive properties while reducing the elastic modulus, leading to favorable outcomes^{8,22}. As most 3D-Ti cages designed before the introduction of PEEK cages are of the window type with a void for bone graft¹⁸, an outstanding research question is whether a non-window-type cage provides a broader contact surface for improved osseointegration. There have been few comprehensive studies comparing clinical and radiographic outcomes between window and non-window-type 3D-Ti cages^{23,24}. Thus, a well-structured randomized controlled trial was needed to fill this knowledge gap.

We hypothesized that non-window-type 3D-Ti cages would yield clinical and radiographic outcomes equivalent to those achieved with window-type 3D-Ti cages in single-level PLIF. Therefore, the objective of the present study was to evaluate the feasibility of the non-window-type cage without a void for bone graft by comparing its clinical and radiographic outcomes to those of the window-type cage.

Materials and Methods

Study Design and Participants

This study was designed as a multicenter, single-blinded, actively controlled randomized clinical trial with 2 parallel groups. Conducted from September 2020 to December 2022, the trial involved 4 experienced orthopaedic surgeons from 4 different academic centers who had a minimum of 10 years of expertise in the spinal surgery field. The trial was approved by the institutional review board of each center and registered with the Clinical Research Information Service (CRIS, KCT0005793, <https://cris.nih.go.kr>).

The study enrolled patients aged 18 to 80 years undergoing single-level PLIF for degenerative disc disease, spinal stenosis, or spondylolisthesis. Exclusion criteria included prior spinal surgery at the same level, spinal infection or malignancy, medication affecting bone metabolism, or contraindications to spinal fusion. Written informed consent was obtained from all participants before enrollment. Collected demographic data included age, sex, height, weight, smoking history, diagnosis, femoral neck bone mineral density (BMD), lowest T-score, osteoporosis treatment history, surgical level, and cage type.

A total of 70 consecutive patients who met the inclusion criteria were enrolled and randomized; 37 patients were assigned to the window-type cage group and 33 patients were assigned to the non-window-type cage group. Five patients in the window group and 4 in the non-window group were lost to follow-up, a drop-out rate of 13%; there were no dropouts related to adverse events. The study included the remaining 61 patients who completed the 12-month follow-up (Fig. 1).

Randomization and Blinding

Patients were randomly assigned in a 1:1 ratio to either the window or the non-window group using computer-generated sequences employing the block randomization method (block

size of 4). The randomization, coded in R version 4.0.0 (R Development Core Team), was managed by a designated investigator with exclusive access. The allocations to the window and non-window groups were revealed to each institution's principal investigator, while the patients and data analysts remained blinded. The surgeons and outcome assessors were not blinded due to the intervention's nature.

Interventions

All patients underwent single-level PLIF surgery performed by experienced spine surgeons following standard procedures. The only difference between the groups was the type of cage used: window or non-window type. After adequate decompression, the intervertebral disc was removed, and end-plate preparation was carefully performed to facilitate fusion. Additionally, 6 mL of extra-cage bone graft, comprising a mixture of locally sourced autologous bone and cancellous allograft chips, was filled into the anterior intervertebral space on each side. The window-type cages were packed with morselized autologous bone graft. To minimize bias, use of fusion-promoting materials such as bone morphogenetic protein-2 (BMP-2) or demineralized bone matrix was strictly prohibited.

Implants

The window and non-window-type cages (Genoss) used in the present study were fabricated using 3D printing technology with a porosity of 88%, diamond-shaped pores, a pore size of 1,100 μm , and an elastic modulus of 1.2 GPa (Fig. 2). The implants had a standardized 11-mm width, 26-mm length, and 4° lordotic angle, whereas the height ranged from 8 to 12 mm according to the patient's needs. The window-type cage, featuring a void, resulted in a bone contact area of 166.6 mm^2 , compared with 203.4 mm^2 for the non-window-type cage.

Outcome Measures

The primary outcome measure was the Oswestry Disability Index (ODI), which was assessed 12 months postoperatively. The secondary outcomes included interbody fusion rate, subsidence rate, the EuroQol-5 Dimensions (EQ-5D), and complications including surgical site infections, dural tears, neurologic deterioration, and medical complications.

Radiographic Evaluation and Determinants of Fusion

Interbody fusion was determined with both stress radiographs and multiaxial computed tomography (CT) scans 12 months postoperatively. Fusion assessment was conducted by 2 independent orthopaedic spine surgeons with 4 and 5 years of experience who were not involved in the study's design or intervention. Fusion was determined on flexion-extension (F-E) stress radiographs by a difference of $<3^\circ$ in the segmental angle (F-E angle). All centers used a standardized stress radiograph protocol for consistent stress application. In this protocol, flexion involved bending forward from the lower back to the maximal point possible while extension required leaning back maximally. Subsidence was defined as >3 mm of cage subsidence from the end plate as seen on radiographs.

The assessment of interbody fusion on multiaxial CT scans was conducted using the following scoring systems^{25,26}. New bone

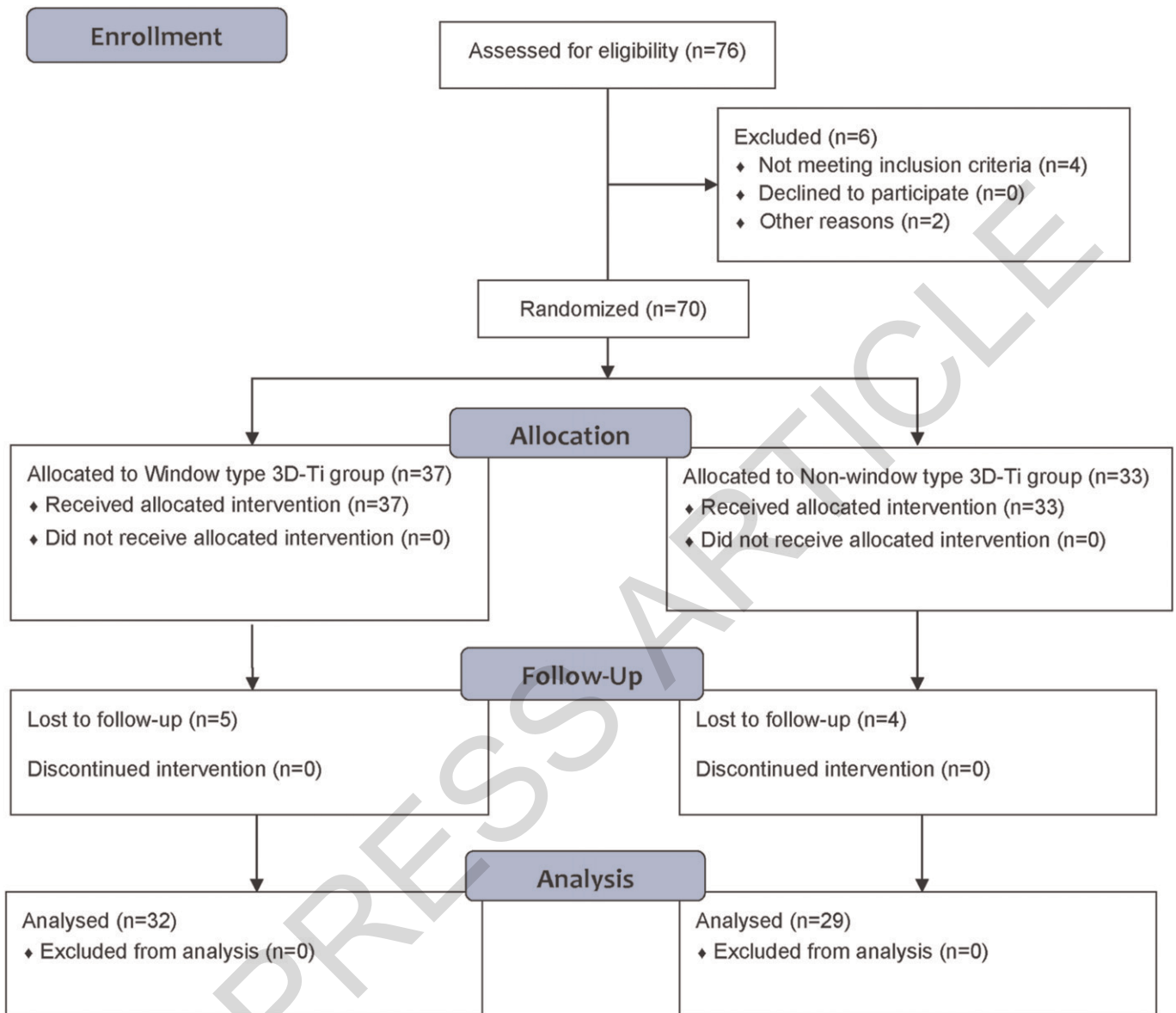


Fig. 1
Consolidated Standards of Reporting Trials (CONSORT) diagram of study enrollment.

formation in the extra-cage space was evaluated using the extra-cage bridging bone (ExCBB) score (Figs. 3-A and 3-B). The ExCBB score assesses new bone formation outside cages (anterior, posterior, intermediate, right, and left) based on bone bridging, with a score of 0 for no bridging, 1 for incomplete bridging, and 2 for complete bridging²⁶. The maximum total ExCBB score for a patient is 10 (2 each for anterior, posterior, intermediate, right, and left). Fusion was deemed to have been achieved when grade-2 bridging was seen in any section.

The intra-cage osseointegration pattern was assessed differently for each group. The window-type group was rated using the intra-cage bridging bone (InCBB) score (Fig. 3-A), rating new bone within the void for bone graft as 0, 1, or 2, on the basis of the same criteria used for the ExCBB score. For the non-window

group, the surface osseointegration ratio (SOR) score²⁵ (Fig. 3-B), which evaluated osseointegration between the cage and the end plates on sagittal CT images, was used. The score was either 0 (radiolucent line along >50% of the end plate) or 1 (integration [no radiolucent line] along >50% of the end plate). The scores for the upper and lower end plates were combined, with a maximum of score of 2, which indicated interbody fusion. To quantitatively compare osseointegration between groups on a numeric scale, the InCBB or SOR scores for the 2 cages in each patient were summed for comparative analysis.

We also looked for the trabecular bone remodeling (TBR) sign, indicating trabecular reaction between the cage-end plate interface and the vertebral body, on coronal CT images (Fig. 4)²⁷.

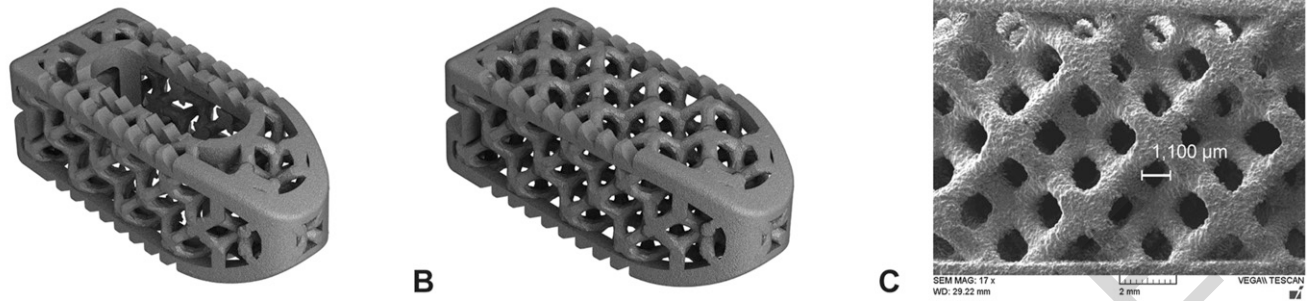


Fig. 2

Two types of 3D-printed porous titanium cages were employed: the window type (**Fig. 2-A**) and non-window type (**Fig. 2-B**). Both cages have a porosity of 88%, diamond-shaped pores, a pore size of 1,100 µm, and an elastic modulus of 1.2 GPa (**Fig. 2-C**). The standardized dimensions of the cages include a width of 11 mm, a length of 26 mm, and a lordotic angle of 4°. The contact areas are 166.6 mm² for the window type and 203.4 mm² for the non-window type. Reproduced with permission from Genoss.

Sample Size Calculation

In the calculation of sample size, the primary outcome measure was the ODI 12 months postoperatively. A successful treatment response was defined as a minimum reduction in the ODI score of 12.8 points, representing the minimal clinically important difference. The sample size calculation was based on separate data from a previous pilot study, not included in the present analysis, setting the standard deviation at 14.3, the power to 90%, the significance level (alpha) to 0.05 for the null hypothesis, and the equivalence margin to 10%. The calculation

suggested a minimum of 56 patients for this 2-treatment parallel design study. To account for a potential dropout rate of 20%, 35 participants were enrolled in each group, resulting in a total sample size of 70 participants.

Statistical Analysis

Baseline characteristics and outcomes were compared between groups using independent t tests for continuous variables and chi-square tests for categorical ones; a 2-sided p value of 0.05 was considered significant. A linear mixed-effects

Extra-cage bone bridging pattern

Intra-cage osteointegration pattern

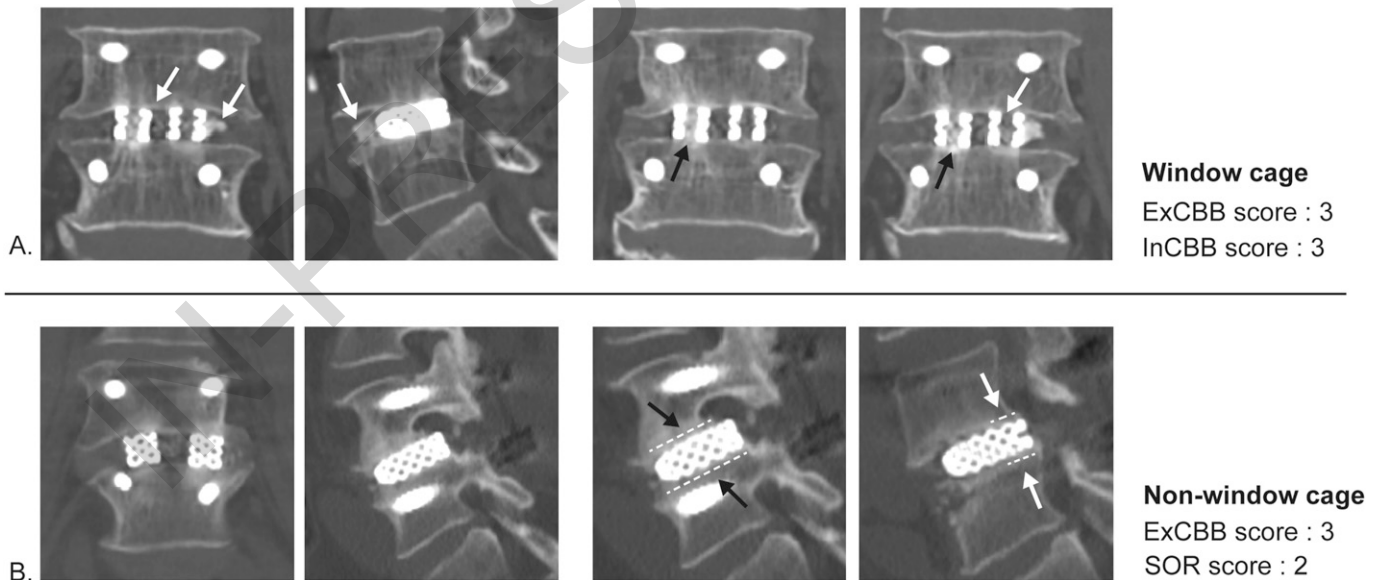


Fig. 3

CT-based scoring systems for interbody fusion assessment. **Fig. 3-A** Intra-cage bridging bone (InCBB) and extra-cage bridging bone (ExCBB) scores were used for the window-type cage group. For both scores, 0 indicates no bridging, 1 (white arrows) represents incomplete or edge-only bridging with a clear radiolucent line, and 2 (black arrows) signifies complete bridging. **Fig. 3-B** The surface osseointegration ratio (SOR) score was used to assess intra-cage osseointegration in the non-window-type cage group. An SOR score of 0 (white arrows) indicates a radiolucent line along >50% of the end plate, while a score of 1 (black arrows) signifies end-plate integration (white dotted lines) along >50% of the end plate without a radiolucent line. The ExCBB score was also used to evaluate extra-cage new bone formation in the non-window cage group.

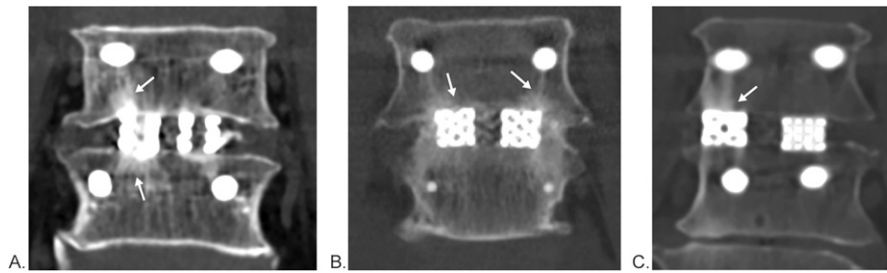


Fig. 4

The trabecular bone remodeling (TBR) sign is shown on CT coronal images both vertically and obliquely, extending from the contact between the cage and vertebral end plate toward the pedicle screw (white arrows), in the window (**Fig. 4-A**) and non-window (**Figs. 4-B and 4-C**) cage groups. The TBR sign indicates the trabecular reaction between the cage-end plate interface and the vertebral body.

model (LMEM) with time points and groups as fixed factors and patients as random effects was used for the primary outcome analysis. Missing data were addressed using an intention-to-treat approach, employing a last observation car-

ried forward method for serial data. Fusion evaluation was based on a per-protocol analysis, limited to patients completing the final follow-up. All analyses were conducted using R version 4.2.2.

TABLE I Demographic Data

	Window Group (N = 32)	Non-Window Group (N = 29)	Total (N = 61)	P Value
Age* (yr)	71.3 ± 6.8	70.4 ± 6.6	70.9 ± 6.7	0.631
Female (no. [%])	15 (46.9)	20 (69.0)	35 (57.4)	0.138
BMI* (kg/m ²)	25.0 ± 3.6	25.2 ± 3.4	25.1 ± 3.4	0.799
BMD* (g/cm ²)	0.721 ± 0.163	0.739 ± 0.149	0.730 ± 0.156	0.667
T-score*	-1.3 ± 1.0	-1.3 ± 1.1	-1.3 ± 1.1	0.965
Smoking (no. [%])	1 (3.1)	0	1 (1.6)	>0.99
Preoperative osteoporosis medication (no. [%])				0.175
None	32 (100)	26 (89.7)	58 (95.1)	
Denosumab	0 (0)	1 (3.4)	1 (1.6)	
Parathyroid hormone	0 (0)	2 (6.9)	2 (3.3)	
Postoperative osteoporosis medication (no. [%])				0.878
None	28 (87.5)	26 (89.7)	54 (88.5)	
Denosumab	2 (6.3)	1 (3.4)	3 (4.9)	
Parathyroid hormone	2 (6.3)	2 (6.9)	4 (6.6)	
Diagnosis (no. [%])				0.423
Stenosis	13 (40.6)	8 (27.6)	21 (34.4)	
Spondylolisthesis	19 (59.4)	21 (72.4)	40 (65.6)	
Operative level (no. [%])				0.981
L3-L4	4 (12.5)	4 (13.8)	8 (13.1)	
L4-L5	22 (68.8)	20 (69.0)	42 (68.9)	
L5-S1	6 (18.8)	5 (17.2)	11 (18.0)	
Cage height (no. [%])				0.616
8 mm	4 (12.5)	1 (3.4)	5 (8.2)	
9 mm	14 (43.8)	16 (55.2)	30 (49.2)	
10 mm	11 (34.4)	9 (31.0)	20 (32.8)	
11 mm	2 (6.3)	1 (3.4)	3 (4.9)	
12 mm	1 (3.1)	2 (6.9)	3 (4.9)	

*The values are given as the mean and standard deviation.

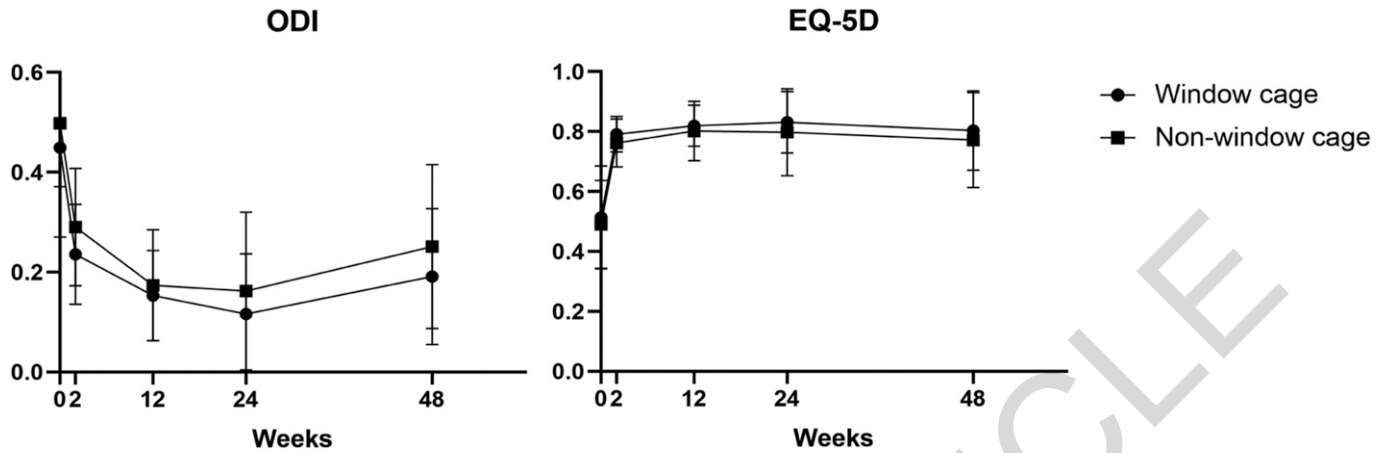


Fig. 5

Linear mixed-effects model analysis indicated no significant differences in the ODI and EQ-5D clinical scores (shown as the mean and standard deviation) between the 2 groups at any time point. Both scores showed significant improvements at 12 months post-surgery in both the window and the non-window group.

Results

Demographics

No significant differences were observed between the groups in terms of age, sex, body mass index (BMI), BMD, lowest T-score, smoking status, or osteoporosis medication (Table I). Additionally, the distribution of operative levels and cage heights showed no significant differences between the groups (Table I).

Clinical Outcomes

The ODI and EQ-5D score showed significant improvements 12 months postoperatively in both groups (Fig. 5) and did

not differ significantly between the groups at any time point (Fig. 5). One dural tear occurred in the window cage group, and 1 superficial infection was reported in the non-window cage group. Neither group experienced any neurologic deterioration or medical complications (Table II).

Radiographic Outcomes

Fusion was achieved in 58 (95.1%) of the 61 patients, and the fusion rate did not differ significantly between the non-window and window cage groups (96.6% and 93.8%, respectively; $p > 0.99$) (Table II). The interobserver reliability of the fusion rating demonstrated a kappa value of 0.792.

TABLE II Clinical and Radiographic Outcomes

	Window Group (N = 32)	Non-Window Group (N = 29)	Total (N = 61)	P Value
Preoperative*				
EQ-5D	0.514 ± 0.172	0.490 ± 0.147	0.503 ± 0.160	0.554
ODI	0.449 ± 0.179	0.498 ± 0.127	0.472 ± 0.157	0.219
12-month postoperative*				
EQ-5D	0.804 ± 0.133	0.772 ± 0.158	0.789 ± 0.145	0.400
ODI	0.191 ± 0.136	0.251 ± 0.164	0.220 ± 0.152	0.133
Surgical site infection (no. [%])	0	1 (3.4)	1 (1.6)	0.960
Dural tear (no. [%])	1 (3.1)	0	1 (1.6)	0.960
Neurologic deterioration (no. [%])	0	0	0	>0.99
Medical complications (no. [%])	0	0	0	>0.99
Successful fusion (no. [%])	30 (93.8)	28 (96.6)	58 (95.1)	>0.99
Segmental angular difference in F-E* (deg)	1.53 ± 1.13	1.59 ± 0.89	1.56 ± 0.102	0.813
Subsidence (no. [%])	5 (15.6)	1 (3.4)	6 (9.8)	0.262
Trabecular bone reaction sign (no. [%])	25 (78.1)	26 (89.7)	51 (83.6)	0.385

*The values are given as the mean and standard deviation.

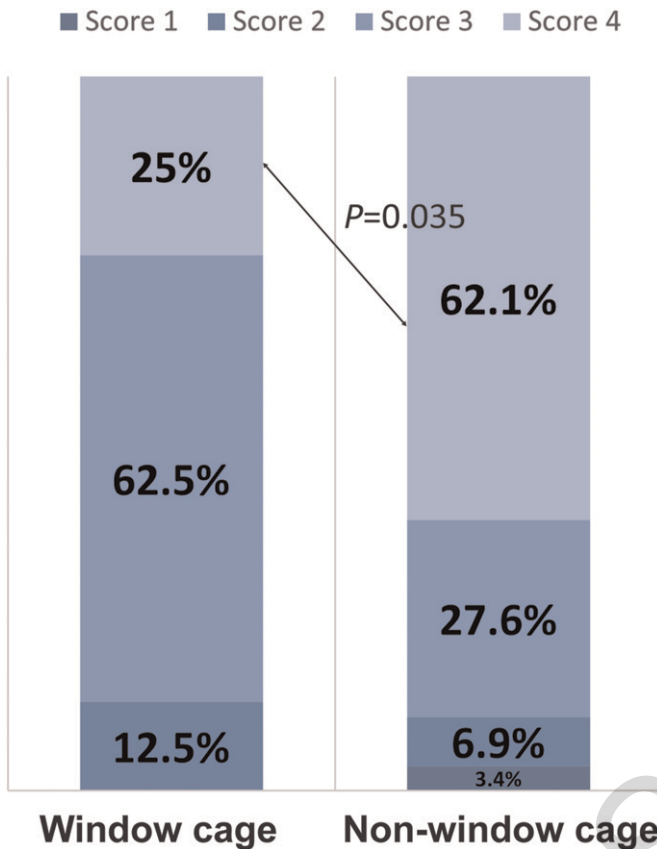


Fig. 6
The percentages of patients with each intra-cage osseointegration score in each group. The non-window group contained a significantly higher proportion of cases with a score of 4 compared with the window cage group ($p = 0.035$ per post hoc analysis).

There was a discrepancy in the classifications of 1 of the 3 nonunions, with the patient eventually classified as having a nonunion following discussion between the assessors. Comparison of the F-E angle between the 2 groups revealed no significant difference (Table II). The subsidence rate also showed no significant difference between the groups, despite

being numerically higher in the window cage group (15.6% versus 3.6%, $p = 0.262$; Table II).

A significant difference was noted in the intra-cage osseointegration scores ($p = 0.007$), with more patients having a score of 4 in the non-window group (Fig. 6, Table III). A TBR was observed in 51 (87.9%) of the 58 patients achieving interbody fusion. The TBR-positive proportion was numerically higher in the non-window cage group across the entire cohort but it was not significantly higher (89.7% versus 78.1%, $p = 0.385$; Table II).

Discussion

The present study demonstrates that both window and non-window types of cages can achieve satisfactory interbody fusion rates that do not differ significantly from one another (93.8% and 96.6%, respectively). Furthermore, at a 12-month follow-up, significant improvement in clinical outcomes was observed in both groups, with no significant differences found between the groups at any time point.

The overall fusion rate of 95% in the present study was in line with previously reported fusion rates of 83% to 100% following PLIF using titanium cages^{28,29}. Interestingly, while the finding was not significant, the fusion rate in the non-window cage group was numerically higher than that in the window cage group. Additionally, intra-cage osseointegration scores differed significantly between the groups ($p = 0.007$), with the non-window group having more cases with a score of 4 than the window cage group (Fig. 6, Table III). This may be due to the non-window cage having a 22% larger contact surface area, enhancing the effect of surface roughness on reducing early postoperative micromotion at the implant-bone interface and providing a stable interface^{30,31}, which minimizes the risk of early implant loosening and failure¹¹.

The wide contact surface can also provide an extensive area for osseointegration between the porous structure and the end plate³². This allows optimization of the unique advantage of the porous-structured titanium cage in promoting osseointegration³³⁻³⁵. Segi et al.²⁷ analyzed CT images and described TBR signs associated with titanium cages as a reactive change to the vertebral body during the osseointegration process. They

TABLE III Intra- and Extra-Cage Osseointegration Scores

	Window Group (N = 32)	Non-Window Group (N = 29)	Total (N = 61)	P Value
ExCBB score*	5.7 ± 1.7	5.6 ± 1.3	5.7 ± 1.5	0.801
Intra-cage osseointegration score† (no. [%])				0.007
0	0	0	0	
1	0 (0.0)	1 (3.4)	1 (1.6)	
2	4 (12.5)	2 (6.9)	6 (9.8)	
3	20 (62.5)	8 (27.6)	28 (45.9)	
4	8 (25.0)	18 (62.1)	26 (42.6)	

*The values are given as the mean and standard deviation. †The new-bone formation within the cage was assessed using the InCBB scoring system for window-type cages and the SOR scoring system for non-window-type cages.

reported higher fusion rates in patients with early postoperative TBR signs. In the present study, the TBR sign was observed in 51 (87.9%) of 58 patients who achieved interbody fusion. Despite the lack of statistical significance, the TBR-positive rate was numerically higher in the non-window cage group across the entire cohort than in the window group (89.7% and 78.1%, respectively; Table II). Furthermore, TBR occurred on the porous surface in the window cages, not where the void for bone graft was present (Fig. 4-A), whereas TBR was observed to be distributed across the surface of the non-window cages (Figs. 4-B and 4-C). Thus, the broad contact surface would have contributed to a favorable radiographic outcome by providing a wider area for osseointegration and thus greater mechanical stability through osseointegration on the cage-end plate interface^{16,36,37}.

Interestingly, the subsidence rate was numerically higher in the window cage group than in the non-window cage group, although not significantly so (15.6% versus 3.4%, $p = 0.262$). This might be due to the reduced elastic modulus resulting from the porous structure in the titanium cage, affecting the overall modulus but not the end-plate contact properties³⁸⁻⁴⁰. A narrow contact surface can concentrate stress, possibly increasing subsidence regardless of the cage's overall modulus. Previous studies^{41,42} have indicated a lower subsidence rate with larger end-plate contact areas, suggesting that the larger contact surface of the non-window cage may offer better support through more uniform stress distribution across the end plate.

In addition to cage design, meticulous end-plate preparation is crucial for preventing subsidence. Overly aggressive end-plate preparation that leads to violation of the cortical bone can increase the risk of subsidence. Therefore, surgeons should aim for careful end-plate preparation, removing the cartilaginous layer while preserving the subchondral bone. Furthermore, understanding the patient's bone quality and tailoring the surgical technique accordingly can reduce the risk of subsidence⁴³. In this context, the use of a non-window-type cage with a larger contact surface can provide additional support, particularly in patients with compromised bone quality.

This study has limitations that should be acknowledged. A major limitation is related to the study design, particularly in the selection of the primary outcome. The postoperative 12-month ODI, which was the primary outcome of the study, may not provide sufficient power to adequately compare the radiographic outcomes, including the fusion rate. However, using the fusion rate as the primary outcome would have required an impractically large sample size to achieve the desired statistical power. Therefore, we opted for a clinical outcome score for equivalence assessment, combined with radiographic outcome analysis to emphasize the potential advantages of the non-window-type

cage. The study could also be limited by the follow-up period of 12 months, which may be insufficient to evaluate the long-term outcomes of the 2 cage types. However, the overall fusion rate of 95.1% is favorable, and we do not believe that the 3 nonunions identified would have substantially impacted the study's main conclusion (equivalency of ODIs) even with a 24-month follow-up. Future studies with larger sample sizes and extended follow-up periods are warranted to expand our findings. It should also be noted that the bone graft type and quantity used in this study might differ from those in other clinical settings. Finally, the impact of fusion-promoting materials such as BMP-2 cannot be ascertained from our study.

In conclusion, the results of this study demonstrate that non-window-type 3D-Ti cages without a void for bone graft can achieve clinical outcomes equivalent to those of window-type 3D-Ti cages and comparable interbody fusion rates. These results suggest that the potential advantages of 3D-Ti cages could be optimized in the absence of a void for bone graft by providing a larger contact surface for osseointegration. ■

Dae-Woong Ham, MD¹
Sang-Min Park, MD²
Youngbae B. Kim, MD³
Dong-Gune Chang, MD⁴
Jae Jun Yang, MD⁵
Byung-Taek Kwon, MD⁶
Kwang-Sup Song, MD¹

¹Department of Orthopedic Surgery, Chung-Ang University Hospital, College of Medicine, Chung-Ang University, Seoul, Republic of Korea

²Spine Center and Department of Orthopaedic Surgery, Seoul National University Bundang Hospital, Seoul National University College of Medicine, Seongnam, Republic of Korea

³Department of Orthopedic Surgery, VHS Medical Center, Seoul, Republic of Korea

⁴Spine Center and Department of Orthopedic Surgery, Inje University Sanggye Paik Hospital, College of Medicine, Inje University, Seoul, Republic of Korea

⁵Department of Orthopedic Surgery, Dongguk University Ilsan Hospital, Goyang, Republic of Korea

⁶Department of Orthopedic Surgery, Chung-Ang University Gwang Myeong Hospital, Gwangmyeong, Republic of Korea

Email for corresponding author; ksong70@cau.ac.kr

References

- Lee JH, Kong CB, Yang JJ, Shim HJ, Koo KH, Kim J, Lee CK, Chang BS. Comparison of fusion rate and clinical results between CaO-SiO₂-P₂O₅-B₂O₃ bioactive glass ceramics spacer with titanium cages in posterior lumbar interbody fusion. *Spine J*. 2016 Nov;16(11):1367-76.
- Norton RP, Bianco K, Klifto C, Errico TJ, Bendo JA. Degenerative Spondylolisthesis: An Analysis of the Nationwide Inpatient Sample Database. *Spine (Phila Pa 1976)*. 2015 Aug 1;40(15):1219-27.
- Rao PJ, Pelletier MH, Walsh WR, Mobbs RJ. Spine interbody implants: material selection and modification, functionalization and bioactivation of surfaces to improve osseointegration. *Orthop Surg*. 2014 May;6(2):81-9.
- Mobbs RJ, Phan K, Malham G, Seex K, Rao PJ. Lumbar interbody fusion: techniques, indications and comparison of interbody fusion options including PLIF, TLIF, MI-TLIF, OLIF/ATP, LLIF and ALIF. *J Spine Surg*. 2015 Dec;1(1):2-18.

5. Cole CD, McCall TD, Schmidt MH, Dailey AT. Comparison of low back fusion techniques: transforaminal lumbar interbody fusion (TLIF) or posterior lumbar interbody fusion (PLIF) approaches. *Curr Rev Musculoskelet Med.* 2009 Jun;2(2):118-26.
6. DiPaola CP, Molinari RW. Posterior lumbar interbody fusion. *J Am Acad Orthop Surg.* 2008 Mar;16(3):130-9.
7. Kim YH, Ha KY, Kim YS, Kim KW, Rhyu KW, Park JB, Shin JH, Kim YY, Lee JS, Park HY, Ko J, Kim SI. Lumbar Interbody Fusion and Osteobiologics for Lumbar Fusion. *Asian Spine J.* 2022 Dec;16(6):1022-33.
8. Seaman S, Kerezoudis P, Bydon M, Torner JC, Hitchon PW. Titanium vs. polyetheretherketone (PEEK) interbody fusion: Meta-analysis and review of the literature. *J Clin Neurosci.* 2017 Oct;44:23-9.
9. Kuslich SD, Ulstrom CL, Griffith SL, Ahern JW, Dowdle JD. The Bagby and Kuslich method of lumbar interbody fusion. History, techniques, and 2-year follow-up results of a United States prospective, multicenter trial. *Spine (Phila Pa 1976).* 1998 Jun 1;23(11):1267-78, discussion 1279.
10. Igarashi H, Hoshino M, Omori K, Matsuzaki H, Nemoto Y, Tsuruta T, Yamasaki K. Factors influencing interbody cage subsidence following anterior cervical discectomy and fusion. *Clin Spine Surg.* 2019 Aug;32(7):297-302.
11. Sundfeldt M, Carlsson LV, Johansson CB, Thomsen P, Gretzer C. Aseptic loosening, not only a question of wear: a review of different theories. *Acta Orthop.* 2006 Apr;77(2):177-97.
12. Pechlivanis I, Thuring T, Brenke C, Seiz M, Thome C, Barth M, Harders A, Schmieder K. Non-fusion rates in anterior cervical discectomy and implantation of empty polyetheretherketone cages. *Spine (Phila Pa 1976).* 2011 Jan 1;36(1):15-20.
13. Panayotov IV, Orti V, Cuisinier F, Yachouh J. Polyetheretherketone (PEEK) for medical applications. *J Mater Sci Mater Med.* 2016 Jul;27(7):118.
14. Brantigan JW, Steffee AD, Geiger JM. A carbon fiber implant to aid interbody lumbar fusion. Mechanical testing. *Spine (Phila Pa 1976).* 1991 Jun;16(6)(Suppl):S277-82.
15. Briem D, Strametz S, Schröder K, Meenen NM, Lehmann W, Linhart W, Ohl A, Rueger JM. Response of primary fibroblasts and osteoblasts to plasma treated polyetheretherketone (PEEK) surfaces. *J Mater Sci Mater Med.* 2005 Jul;16(7):671-7.
16. Torstrick FB, Lin ASP, Safranski DL, Potter D, Sulchek T, Lee CSD, Gall K, Guldborg RE. Effects of surface topography and chemistry on polyether-ether-ketone (PEEK) and titanium osseointegration. *Spine (Phila Pa 1976).* 2020 Apr 15;45(8):E417-24.
17. Olivares-Navarrete R, Gittens RA, Schneider JM, Hyzy SL, Haithcock DA, Ullrich PF, Schwartz Z, Boyan BD. Osteoblasts exhibit a more differentiated phenotype and increased bone morphogenetic protein production on titanium alloy substrates than on poly-ether-ether-ketone. *Spine J.* 2012 Mar;12(3):265-72.
18. Muthiah N, Yolcu YU, Alan N, Agarwal N, Hamilton DK, Ozpinar A. Evolution of polyetheretherketone (PEEK) and titanium interbody devices for spinal procedures: a comprehensive review of the literature. *Eur Spine J.* 2022 Oct;31(10):2547-56.
19. Ducheyne P, Qiu Q. Bioactive ceramics: the effect of surface reactivity on bone formation and bone cell function. *Biomaterials.* 1999 Dec;20(23-24):2287-303.
20. Fujibayashi S, Neo M, Kim HM, Kokubo T, Nakamura T. Osteoinduction of porous bioactive titanium metal. *Biomaterials.* 2004 Feb;25(3):443-50.
21. Hasegawa T, Ushirozako H, Shigeto E, Ohba T, Oba H, Mukaiyama K, Shimizu S, Yamato Y, Ide K, Shibata Y, Ojima T, Takahashi J, Haro H, Matsuyama Y. The titanium-coated PEEK cage maintains better bone fusion with the endplate than the PEEK cage 6 months after PLIF surgery: a multicenter, prospective, randomized study. *Spine (Phila Pa 1976).* 2020 Aug 1;45(15):E892-902.
22. McGilvray KC, Easley J, Seim HB, Regan D, Berven SH, Hsu WK, Mroz TE, Puntlitz CM. Bony ingrowth potential of 3D-printed porous titanium alloy: a direct comparison of interbody cage materials in an in vivo ovine lumbar fusion model. *Spine J.* 2018 Jul;18(7):1250-60.
23. Laratta JL, Vivace BJ, López-Peña M, Guzmán FM, Gonzalez-Cantalpeidra A, Jorge-Mora A, Villar-Liste RM, Pino-Lopez L, Lukyanchuk A, Taghizadeh EA, Pino-Minguez J. 3D-printed titanium cages without bone graft outperform PEEK cages with autograft in an animal model. *Spine J.* 2022 Jun;22(6):1016-27.
24. Fujibayashi S, Takemoto M, Ishii K, Funao H, Isogai N, Otsuki B, Shimizu T, Nakamura T, Matsuda S. Multicenter Prospective Study of Lateral Lumbar Interbody Fusions Using Bioactive Porous Titanium Spacers without Bone Grafts. *Asian Spine J.* 2022 Dec;16(6):890-7.
25. Ham DW, Jung CW, Chang DG, Yang JJ, Song KS. Feasibility of non-window three-dimensional-printed porous titanium cage in posterior lumbar interbody fusion: a pilot trial. *Clin Orthop Surg.* 2023 Dec;15(6):960-7.
26. Lee J, Lee DH, Jung CW, Song KS. The significance of extra-cage bridging bone via radiographic lumbar interbody fusion criterion. *Global Spine J.* 2023 Jan;13(1):113-21.
27. Segi N, Nakashima H, Shinjo R, Kagami Y, Ando K, Machino M, et al. Trabecular bone remodeling as a new indicator of osteointegration after posterior lumbar interbody fusion. *Global Spine J.* 2024 Jan;14(1):25-32.
28. Tanida S, Fujibayashi S, Otsuki B, Masamoto K, Takahashi Y, Nakayama T, Matsuda S. Vertebral endplate cyst as a predictor of nonunion after lumbar interbody fusion: comparison of titanium and polyetheretherketone cages. *Spine (Phila Pa 1976).* 2016 Oct 15;41(20):E1216-22.
29. Nemoto O, Asazuma T, Yato Y, Imabayashi H, Yasuoka H, Fujikawa A. Comparison of fusion rates following transforaminal lumbar interbody fusion using polyetheretherketone cages or titanium cages with transpedicular instrumentation. *Eur Spine J.* 2014 Oct;23(10):2150-5.
30. Stadelmann VA, Terrier A, Pioletti DP. Microstimulation at the bone-implant interface upregulates osteoclast activation pathways. *Bone.* 2008 Feb;42(2):358-64.
31. Lewis G. Properties of open-cell porous metals and alloys for orthopaedic applications. *J Mater Sci Mater Med.* 2013 Oct;24(10):2293-325.
32. Gittens RA, Olivares-Navarrete R, Schwartz Z, Boyan BD. Implant osseointegration and the role of microroughness and nanostructures: lessons for spine implants. *Acta Biomater.* 2014 Aug;10(8):3363-71.
33. Chang B, Song W, Han T, Yan J, Li F, Zhao L, Kou H, Zhang Y. Influence of pore size of porous titanium fabricated by vacuum diffusion bonding of titanium meshes on cell penetration and bone ingrowth. *Acta Biomater.* 2016 Mar;33:311-21.
34. Swaminathan PD, Uddin MN, Wooley P, Asmatulu R. Fabrication and biological analysis of highly porous PEEK bionanocomposites incorporated with carbon and hydroxyapatite nanoparticles for biological applications. *Molecules.* 2020 Aug 6;25(16):3572.
35. Torstrick FB, Lin ASP, Potter D, Safranski DL, Sulchek TA, Gall K, Guldborg RE. Porous PEEK improves the bone-implant interface compared to plasma-sprayed titanium coating on PEEK. *Biomaterials.* 2018 Dec;185:106-16.
36. Makino T, Kaito T, Sakai Y, Takenaka S, Yoshikawa H. Computed tomography color mapping for evaluation of bone ongrowth on the surface of a titanium-coated polyetheretherketone cage in vivo: A pilot study. *Medicine (Baltimore).* 2018 Sep;97(37):e12379.
37. Guyer RD, Abitbol JJ, Ohnmeiss DD, Yao C. Evaluating osseointegration into a deeply porous titanium scaffold: a biomechanical comparison with PEEK and allograft. *Spine (Phila Pa 1976).* 2016 Oct 1;41(19):E1146-50.
38. Li F, Li J, Kou H, Huang T, Zhou L. Compressive mechanical compatibility of anisotropic porous Ti6Al4V alloys in the range of physiological strain rate for cortical bone implant applications. *J Mater Sci Mater Med.* 2015 Sep;26(9):233.
39. Zhang Z, Li H, Fogel GR, Xiang D, Liao Z, Liu W. Finite element model predicts the biomechanical performance of transforaminal lumbar interbody fusion with various porous additive manufactured cages. *Comput Biol Med.* 2018 Apr 1;95:167-74.
40. Li F, Li J, Xu G, Liu G, Kou H, Zhou L. Fabrication, pore structure and compressive behavior of anisotropic porous titanium for human trabecular bone implant applications. *J Mech Behav Biomed Mater.* 2015 Jun;46:104-14.
41. Marchi L, Abdala N, Oliveira L, Amaral R, Coutinho E, Pimenta L. Radiographic and clinical evaluation of cage subsidence after stand-alone lateral interbody fusion. *J Neurosurg Spine.* 2013 Jul;19(1):110-8.
42. Agarwal N, White MD, Zhang X, Alan N, Ozpinar A, Salvetti DJ, Tempel ZJ, Okonkwo DO, Kanter AS, Hamilton DK. Impact of endplate-implant area mismatch on rates and grades of subsidence following stand-alone lateral lumbar interbody fusion: an analysis of 623 levels. *J Neurosurg Spine.* 2020 Mar 6;33(1):12-6.
43. Polikeit A, Ferguson SJ, Nolte LP, Orr TE. The importance of the endplate for interbody cages in the lumbar spine. *Eur Spine J.* 2003 Dec;12(6):556-61.